VOLUME 118, NUMBER 19
MAY 15, 1996

JOURNAL OF THE AMERICAN CHEMICAL SOCIETY

Identification of Conformational Substates in Oxymyoglobin through the pH-Dependence of the Low-Temperature Photoproduct Yield

Lisa M. Miller,‡ Mehul Patel, and Mark R. Chance*

Contribution from the Department of Physiology and Biophysics, Albert Einstein College of Medicine of Yeshiva University, Bronx, New York 10461

Received July 28, 1995⊗

Abstract: The effect of pH on the inner barrier to oxygen binding in myoglobin has been examined through a study of the pH-dependence of the low-temperature photoproduct yield for horse oxymyoglobin (MbO_2). Chance et al. (Chance, M. R.; Courtney, S. H.; Chavez, M. D.; Ondrias, M. R.; Friedman, J. M. *Biochemistry* **1990**, *29*, 5537) have shown that the low-temperature photoproduct yield of MbO_2 is 0.50 ± 0.05 and have suggested the existence of two conformational substates, where the "photolyzable" fraction has a barrier similar to MbCO and the "unphotolyzable" fraction represents a very low barrier or barrierless substate. Through optical spectroscopy, we show that the 10 K photoproduct yield decreases at low pH for MbO_2 (pH 7: 0.50 ± 0.05; pH 5: 0.18 ± 0.05) and cobalt-substituted MbO_2 (pH 7: 0.55 ± 0.05; pH 4: 0.20 ± 0.05), indicating distal pocket conformational changes that occur as pH is lowered which further populate a low barrier conformation. A comparison of the pH-dependence of (1) the MbO_2 photoproduct yield and (2) the A state population of carbonmonoxy myoglobin (MbCO) at cryogenic temperatures indicates that the conformational changes that give rise to the $A_1 \rightarrow A_0$ conformational substate transition in MbCO are functionally important in determining the inner barrier to oxygen binding. The pH-dependence of the $A_1 \rightarrow A_0$ state transition in MbCO has been attributed to protonation of the distal histidine, suggesting that the distal histidine also determines the conformational substate population in MbO_2, hence, the overall inner rebinding barrier. Further support of this theory comes from the photoproduct yield of the mutant, $Mb(H64Q)O_2$, where the hydrogen bond to the distal glutamine does not titrate with pH, which remains constant (0.50 ± 0.05) from pH 4.8 to 9. The pH-dependence of the MbO_2 substate population may be structural or electronic in nature. Structurally, the pH-dependence of the distal pocket environment may lead to different ligand trajectories upon photolysis, affecting the barrier to rebinding. Electronically, the changes that occur in the distal pocket at low pH may cause a redistribution of electron density throughout the metal−porphyrin π-electron system, yielding a fast-relaxing photoexcited state where the Fe−O bond is not ruptured. Finally, the pH versus photoproduct yield "titration curve" for oxymyoglobin was compared to cobalt-substituted oxymyoglobin ($CoMbO_2$). We found a higher apparent pK for MbO_2 than $CoMbO_2$, indicating that protonation of the distal histidine is easier in ferrous oxymyoglobin. These results show direct communication between the π-system of the metal and that of the distal histidine residue, and suggest a stronger hydrogen bond to the distal histidine in MbO_2 versus $CoMbO_2$.

Introduction

The rate of oxygen association in myoglobin (k_{on}) reflects the overall barrier to oxygen binding. This barrier involves (1) diffusion of the ligand through the protein matrix, i.e. the *outer barrier*, and (2) reaction of the ligand with the heme, i.e. the

* Author to whom correspondence should be addressed. Phone: (718) 430-4136. Internet: mrc@aecom.yu.edu.

‡ Present address: Division of Energy and Environment, Lawrence Berkeley National Laboratory, M.S. 2-300, 1 Cyclotron Road, Berkeley, CA 94720.

⊗ Abstract published in *Advance ACS Abstracts,* April 15, 1996.

S0002-7863(95)02534-0 CCC: $12.00

inner barrier.[1,2] Room temperature flash photolysis and recombination studies have shown that the outer barriers for diatomic ligands such as CO, O_2, and NO are similar, and the variations in k_{on} for MbCO, MbO_2, and MbNO arise from different inner barriers to ligand binding.[1,3,4] For O_2 binding, the heights of the inner and outer barriers are approximately equal at neutral pH, whereas for CO binding, the inner barrier is noticeably higher.[1]

Early work by Frauenfelder and co-workers[5] has shown that the inner rebinding barrier can be isolated by flash photolysis of the ligand at cryogenic temperatures, where the protein matrix is frozen and the ligand is unable to escape from the distal pocket. Chance et al.[6] have proposed a direct relationship between the inner barrier to ligand binding and the fraction of ligand-bound material that is converted to "deoxy-like" photoproduct upon photolysis at cryogenic temperatures, i.e. the *photoproduct yield*. In other words, higher inner barriers to ligand binding are reflected in higher observable photoproduct yields at low temperature. Typically, those photoproduct species which survive on nanosecond to longer time scales at room temperature appear "photolyzable" at cryogenic temperatures.

For MbCO, the low-temperature photoproduct yield is 1.0, indicating a photoproduct population with a high barrier to rebinding. This is consistent with room temperature kinetics, which indicate that photolysis of MbCO is complete and the CO ligand rebinds on a microsecond time scale. Conversely, the photoproduct yield of MbO_2 at 8 K is 0.50 ± 0.05. Chance et al. have proposed that the low photoproduct yield of MbO_2 at cryogenic temperatures is due to two structural populations, one with a very low barrier to ligand binding and a second which is similar to MbCO. This two-population hypothesis is supported by room temperature kinetics by Petrich et al.,[7] which have shown two distinct rebinding populations for MbO_2—one which rebinds on a nanosecond time scale and a second that rebinds on a sub-picosecond time scale. It is the fast (sub-picosecond) rebinding population that is thought to be the "unphotolyzable" MbO_2 fraction at cryogenic temperatures. Structurally, the two populations are thought to differ in their proximal environments, where the fast-rebinding species has a more planar heme configuration in the photoproduct state.

In addition to ligand-specific proximal differences in the rebinding intermediates, more recently it has become evident that the structure of the distal pocket also plays an important role in controlling the inner barrier to ligand binding in myoglobin. The stretching frequency of the CO ligand, ν(C−O), is a sensitive probe of structural and electronic variations among different distal pocket conformations. Sperm whale MbCO has been shown to have several ligand-bound conformational substates (A states) with respect to the CO stretching frequency,[8−10] where each conformational substate has unique rebinding kinetics. Substate populations are influenced by many factors, such as pH, temperature, pressure, solvent, and myoglobin species.[9,11−14] The A states arise from different distal pocket conformations that influence the degree of π-back-bonding in MbCO.[15,16] Polar interactions between the O($\delta-$) atom of CO and polar ($\delta+$) distal pocket residues tend to increase back-bonding, which decreases ν(C−O). The pH-dependence of the A states in MbCO has been attributed to distal pocket conformational changes associated with the titration of the distal histidine.[11,13,17,18]

To date, it is unclear whether similar conformational substates exist with respect to the dioxygen stretching frequency in MbO_2 and, if so, whether they influence the inner barrier to oxygen binding. It has been well-established that the distal histidine forms a hydrogen bond with the dioxygen ligand at neutral pH. The electronic structure of the metal−dioxygen moiety (M−O−O) and its interaction with the distal pocket residues play an important role in determining the strength of this hydrogen bond, which, in turn, regulates oxygen affinity. It has been suggested that the hydrogen bond may be ruptured at low pH as the distal histidine swings out of the heme pocket toward the solvent. This conformational change could have a dramatic effect on the barrier to oxygen binding.

This paper addresses the issue of distal pocket conformational substates in MbO_2 and their role in distal control of the inner barrier to oxygen binding in myoglobin. By studying the pH-dependence of the photoproduct yields of MbO_2, $CoMbO_2$, and $Mb(H64Q)O_2$, we examine (1) how titrating amino acid residues in the distal pocket affect the inner barrier to oxygen binding and (2) how the metal center influences these titrating residues. We probe distal pocket structure by studying the A state population in MbCO as a function of pH. These results are compared to the pH-dependence of the MbO_2 photoproduct yields as a means of identifying distal pocket conformational substates in MbO_2 that function in controlling the inner barrier to oxygen binding in myoglobin. Finally, a comparison of the pH-dependence of the photoproduct yields of MbO_2 to $CoMbO_2$ demonstrates a communication between the porphyrin π-system and that of the distal residue. Differences in the electron density distribution throughout the M−O−O···HN−His moieties in MbO_2 versus $CoMbO_2$ can help to explain the differences in oxygen affinity between these two species.

Experimental Section

Preparation of Myoglobin Samples. Horse skeletal muscle myoglobin (95−100%, Sigma) was dissolved in water and stirred on ice for 10 min. Samples were centrifuged for 20 min at 15000 rpm at 10 °C and then transferred to a nitrogen-purged glovebox. A 5-fold excess of sodium dithionite (Aldrich) was added to reduce the iron to the Fe^{II}

(1) Carver, T. E.; Rohlfs, R. J.; Olson, J. S.; Gibson, Q. H.; Blackmore, R. S.; Springer, B. A.; Sligar, S. G. *J. Biol. Chem.* **1990**, *265*, 20007.
(2) Quillin, M. L.; Li, T.; Olson, J. S.; Phillips, G. N.; Dou, Y.; Ikeda-Saito, M.; Regan, R.; Carlson, M.; Gibson, Q. H.; Li, H.; Elber, R. *J. Mol. Biol.* **1995**, *245*, 416.
(3) Doster, W.; Beece, D.; Bowne, S. F.; Dilorio, E. E.; Eisenstein, L.; Frauenfelder, H.; Reinisch, L.; Shyamsunder, E.; Winterhalter, K. H.; Yue, K. T. *Biochemistry* **1982**, *21*, 4831.
(4) Gibson, Q. H.; Regan, R.; Elbers, R.; Olson, J. S.; Carver, T. E. *J. Biol. Chem.* **1992**, *267*, 22022.
(5) Austin, R. H.; Beeson, K.; Eisenstein, L.; Frauenfelder, H.; Gunsalus, I. C. *Biochemistry* **1975**, *14*, 5355.
(6) Chance, M. R.; Courtney, S. H.; Chavez, M. D.; Ondrias, M. R.; Friedman, J. M. *Biochemistry* **1990**, *29*, 5537.
(7) Petrich, J.; Poyart, C.; Martin, J. *Biochemistry* **1988**, *27*, 4049.
(8) Alben, J. O.; Beece, D.; Bowne, S. F.; Doster, W.; Eisenstein, L.; Frauenfelder, H.; Good, D.; McDonald, J. D.; Marden, M. C.; Moh, P. P.; Reinisch, L.; Reynolds, A. H.; Shyamsunder, E.; Yue, K. T. *Proc. Natl. Acad. Sci. U.S.A.* **1982**, *79*, 3744.
(9) Ansari, A.; Berendzen, J.; Braunstein, D.; Cowen, B. R.; Fraunfelder, H.; Hong, M. K.; Iben, I. E. T.; Johnson, J. B.; Ormos, P.; Sauke, T. B.; Scholl, R.; Schulte, A.; Steinbach, P. J.; Vittitow, J.; Young, R. D. *Biophys. Chem.* **1987**, *26*, 337.
(10) Chance, M. R.; Campbell, B. F.; Hoover, R.; Friedman, J. M. *J. Biol. Chem.* **1987**, *262*, 6959.
(11) Fuchsman, W. H.; Appleby, C. A. *Biochemistry* **1979**, *18*, 1309.
(12) Shimada, H.; Caughey, W. S. *J. Biol. Chem.* **1982**, *257*, 11893.
(13) Morikis, D.; Champion, P. M.; Springer, B. A.; Sligar, S. G. *Biochemistry* **1989**, *28*, 4791.
(14) Hong, M. K.; Braunstein, D.; Cowen, B.; Frauenfelder, H.; Iben, I. E. T.; Mourant, J. R.; Ormos, P.; Scholl, R.; Schulte, A.; Steinback, P. J.; Xie, A.; Young, R. D. *Biophys. J.* **1990**, *58*, 429.
(15) Ray, G. B.; Li, X. Y.; Ibers, J. A.; Sessler, J. L.; Spiro, T. G. *J. Am. Chem. Soc.* **1994**, *116*, 162.
(16) Hu, S.; Vogel, K. M.; Spiro, T. G. *J. Am. Chem. Soc.* **1994**, *116*, 11187.
(17) Hayashi, Y.; Yamada, H.; Yamazaki, I. *Biochim. Biophys. Acta* **1976**, *427*, 608.
(18) Tian, W. D.; Sage, J. T.; Champion, P. M. *J. Mol. Biol.* **1993**, *233*, 155.

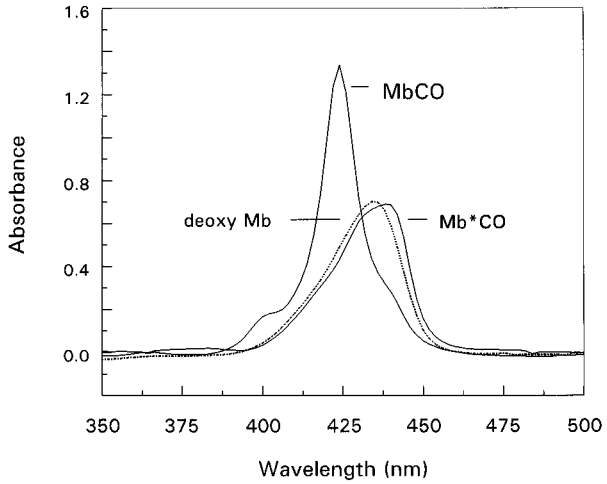

Figure 1. Optical spectra at 8 K for MbCO, Mb*CO, and deoxy Mb at pH 7. The MbCO and deoxy Mb samples were 2 mM in 100 mM potassium phosphate buffer. The solvent was 75:25 by volume glycerol/buffer and the sample path length was 0.005 cm. MbCO was photolyzed at 10 K for 5 min per side with a high-intensity white light source.

state. After the mixture was stirred for 10 min, oxygen (99 atom %, MG Industries) or carbon monoxide (99.5 atom %, MG Industries) was blown over the sample for 10 min. Optical spectra indicated the samples to be greater than 95% oxy- or carbonmonoxy myoglobin. Cobalt-substituted oxymyoglobin was a gift from Dr. H. C. Lee and was prepared from horse skeletal muscle myoglobin as described previously.[19] The site-directed mutant Mb(H64Q)O_2 was obtained from Dr. M. Ikeda-Saito and was prepared from human myoglobin following published methods.[20]

Methods for Determining Low-Temperature Photoproduct Yields. Concentrated MbO_2, $CoMbO_2$, or Mb(H64Q)O_2 (7−8 mM in water) was diluted into buffer (150 mM potassium phosphate, sodium citrate, or sodium acetate in 75:25 glycerol/water) to give a final concentration on the order of 1.5 mM. Samples were placed between two CaF_2 windows using a 0.050-mm Teflon spacer, yielding an optical density in the Soret region between 0.8 and 1.0 OD. The sample holder was mounted in a low-temperature cryostat (Janis ST-4B) which was interfaced to a Lakeshore Temperature Controller (Model 805). Samples were cooled via a liquid helium transfer line. Spectra were taken using a Hewlett Packard Diode Array Spectrometer (Model HP8452A). Data collection time was 0.1 s for each spectrum to prevent photolysis of the sample by the spectrometer's deuterium source lamp. The sample was cooled to 8 K and a spectrum of the ligand-bound MbO_2 was taken. Then, the sample was photolyzed for 5 min per side using a high-intensity white light source (CUDA Products, Inc. Model I-150) or by a 2-min exposure to the spectrometer's deuterium lamp. Both photolysis sources yielded the same results, and longer exposure times did not increase the degree of photolysis. The photolysis protocol was first tested with an MbCO sample, which has a photoproduct yield of 1.0 (Figure 1).[6] We were able to achieve 100% photolysis of the MbCO with a 2 min per side illumination by the white-light source or a 40 s exposure to the spectrometer source lamp. After photolysis, the light source was turned off and spectra of the photolyzed sample (Mb*O_2) were taken at 10 K increments as the sample was warmed—until it had fully recombined. Second-derivative analysis revealed two components in the Mb*O_2 spectrum.

Photoproduct yields are defined as the amount of ligand-bound material that is converted to a "deoxy-like" photoproduct at cryogenic temperatures. They were determined by interactively subtracting a variable fraction of the 8 K ligand-bound spectrum (MbO_2) from the 8 K photolyzed spectrum (Mb*O_2) until the contribution to the difference spectrum at the peak wavelength of the ligand-bound spectrum was zero (i.e. at 418 nm for MbO_2 and 426 nm for $CoMbO_2$) (Figure 2). The value of the variable fraction that satisfies this condition was the

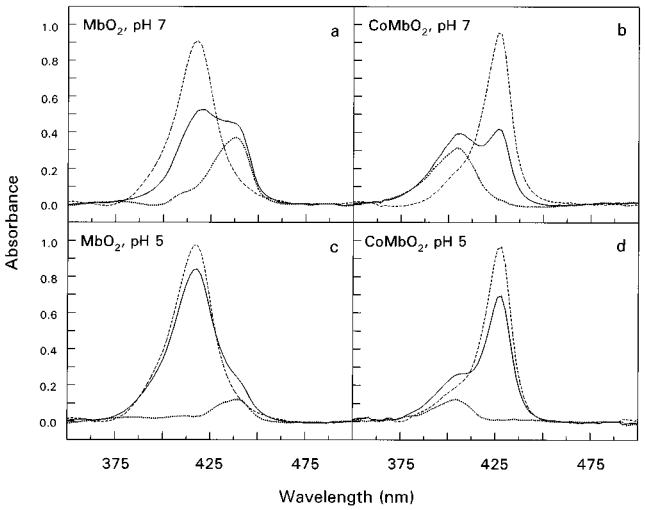

Figure 2. Optical spectra at 8 K for MbO_2 (- - -), Mb*O_2 (—), and Mb* + O_2 (•••) at (a) pH 7 and (b) pH 5 and for $CoMbO_2$ (- - -), CoMb*O_2 (—), and CoMb* + O_2 (···) at (c) pH 7 and (d) pH 5. Sample concentrations were 1.4 mM. The solvent was 75:25 by volume glycerol/buffer, where the buffer concentration was 100 mM potassium phosphate. The path length was 0.005 cm. Samples were photolyzed as described in Figure 1.

fraction of ligand-bound material that remained in the Mb*O_2 spectrum after photolysis. Therefore, the photoproduct yield was obtained by subtracting that fraction from 1.0. The difference spectrum that remained after subtracting (1 − QY)MbO_2 from Mb*O_2 was that of the MbO_2 photoproduct (Mb* + O_2).

FTIR Methods for Determining MbCO Substates. The FTIR spectrometer was thoroughly purged with nitrogen gas for 2 h prior to collecting data, to remove all water vapor and CO_2 from the infrared beam path. The spectrometer was considered sufficiently purged when the ratio of two consecutive "air" spectra yielded a noise spectrum with a peak-to-peak ratio of 10^{-5} OD units. Horse skeletal muscle MbCO samples (2−5 mM in 150 mM potassium phosphate buffer in 75:25 glycerol/water by volume) were placed between two CaF_2 windows using a 0.025-mm Teflon spacer and mounted into an N_2-purged, low-temperature cryostat (Janis ST-4B). Samples were cooled to 220 K with liquid nitrogen. Then the cryostat was evacuated to 50 mT and the samples were cooled further.

Spectral interferograms (128 scans) were collected on a Mattson Galaxy 5000 FTIR spectrometer from 900 to 4000 cm^{-1} with 2-cm^{-1} resolution and Fourier transformed using FIRST software provided by Mattson, Inc. Spectra were generated by dividing each MbCO spectrum by an "air spectrum" and converting from transmittance to absorbance units. Using Spectra Calc software (Galactic Industries), the spectra were fitted to a cubic polynomial baseline in the region from 1900 to 2000 cm^{-1} and the A state CO stretch bands were integrated. The A_1 state fraction was determined by dividing the integrated area of the A_1 band by the total integrated area of A_1 and A_0, i.e. $A_1/(A_1 + A_0)$.

Results

pH-Dependence of the MbO_2 and Mb(H64Q)O_2 Photoproduct Yield. Figure 2 shows the 8 K optical spectra of ligand-bound (MbO_2), photolyzed (Mb*O_2), and the deduced photoproduct (Mb* + O_2) of oxymyoglobin at pH 7 versus pH 5. Ligand-bound MbO_2 is composed of a single peak with a maximum at 418 nm. Second-derivative analysis of the Mb*O_2 spectra revealed two components—one with a maximum at the position of ligand-bound MbO_2 and the second with a maximum at the position of deoxy Mb. The Mb* + O_2 spectrum at pH 7 was obtained by subtracting 0.50MbO_2 from the Mb*O_2 spectrum. This result indicates that 50% of the Mb*O_2 spectrum is due to ligand-bound MbO_2, indicating a photolysis quantum yield of 0.50 ± 0.05. In the same fashion, the Mb* + O_2

(19) Yonetani, T.; Yamamato, H.; Woodrow, G. V., III *J. Biol. Chem.* **1974**, *249*, 682.

(20) Springer, B. A.; Sligar, S. G. *Proc. Natl. Acad. Sci. U.S.A.* **1987**, *84*, 8961.

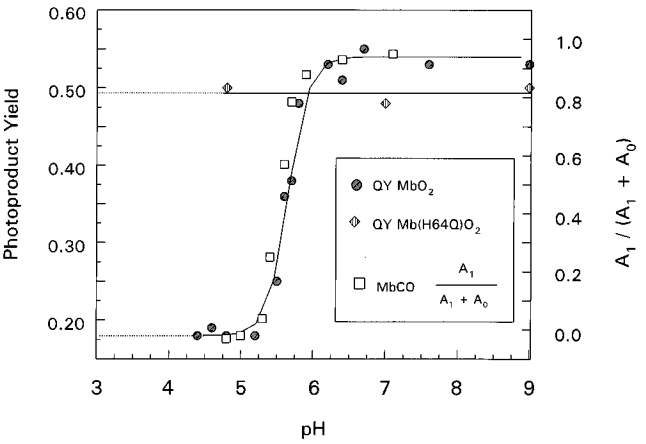

Figure 3. pH-dependence of the low-temperature photoproduct yield for MbO_2 and the mutant, Mb(H64Q)O_2. Photoproduct yields were determined as described in the text. Open squares represent the fraction of A_1 state for horse skeletal muscle MbCO versus pH at 150 K. To verify sample pH at cryogenic temperatures, potassium phosphate, sodium citrate, and sodium acetate buffers were all tested and found to give the same photoproduct yields.

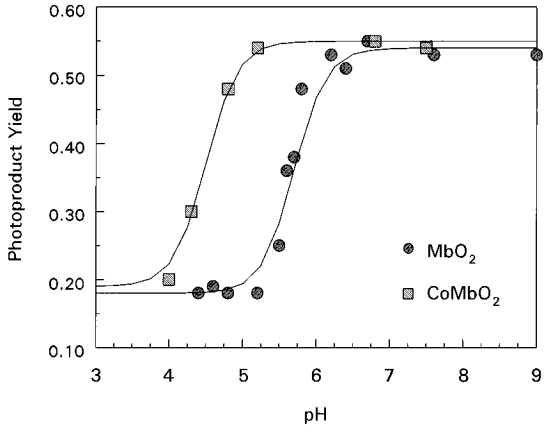

Figure 4. pH-dependence of the low-temperature photoproduct yield for MbO_2 versus $CoMbO_2$. Photoproduct yields were determined as described in the text.

spectrum at pH 5 was obtained by subtracting 0.82MbO_2 from the Mb*O_2 spectrum, indicating a photoproduct yield of 0.18 ± 0.05.

A plot of photoproduct yield versus pH (filled circles in Figure 3) clearly demonstrates that the low-temperature quantum yield of photolysis decreases at low pH for MbO_2 (pH 7: 0.50 ± 0.05; pH 5: 0.18 ± 0.05), suggesting that pH strongly alters the inner oxygen rebinding barrier. It appears that this effect is centered on the protonation of the distal histidine; the photoproduct yield of the mutant, Mb(H64Q)O_2, where the hydrogen bond to the distal glutamine[21] does not titrate with pH, remains constant (0.50 ± 0.05) from pH 4.8 to 9 (filled diamonds in Figure 3). To verify sample pH at cryogenic temperatures, sodium citrate and sodium acetate buffers were also used and found to give the same photoproduct yields.

pH-Dependence of the $CoMbO_2$ Photoproduct Yield. The pH-dependence of the low-temperature photoproduct yield for cobalt-substituted oxymyoglobin can be seen in Figures 2 and 4. Both the maximum photoproduct yield (MbO_2: 0.50 ± 0.05; $CoMbO_2$: 0.55 ± 0.05) and the minimum photoproduct yield (MbO_2: 0.18 ± 0.05; $CoMbO_2$: 0.20 ± 0.05) are the same and the shape of the $CoMbO_2$ titration curve strongly resembles that of MbO_2. One obvious difference exists between the $CoMbO_2$ and MbO_2 titration curves: The apparent p*K* of this titration curve for $CoMbO_2$ is 4.6, which is considerably lower than that for native MbO_2. This shift implies a difference in the distal pocket environments for the two species. More specifically, a lower apparent p*K* for $CoMbO_2$ indicates that protonation of the δ-nitrogen of the distal histidine is more difficult than for MbO_2. This may indicate different distal-side hydrogen bond strengths between MbO_2 and $CoMbO_2$.

Discussion

Chance et al. have shown that the photoproduct yield of MbO_2 at cryogenic temperatures is 0.50 ± 0.05, attributable to two structural populations with different inner barriers to rebinding.[6,22] The "photolyzable" fraction represents a "deoxy-like" photoproduct state, similar to the MbCO photoproduct. The "unphotolyzable" fraction arises from a photoproduct state with very little or no barrier to recombination. Structurally, the barrier height difference between the two states has been attributed to different proximal environments, where the low-barrier photoproduct state has a more planar heme. In addition, however, the data we present suggest that the population of this low-barrier species is pH-dependent, and thus appears to (also) be influenced by the distal pocket conformation.

Many infrared studies of MbCO have demonstrated that the CO stretching frequency provides a good spectroscopic probe of the distal pocket environment. Sperm whale MbCO exhibits three conformational substates with respect to the CO stretching frequency denoted by A_0 (1966 cm^{-1}), A_1 (1945 cm^{-1}), and A_3 (1930 cm^{-1}).[9,10,14] Substate populations are dependent on temperature, pH, pressure, solvent, and myoglobin source.[9−14] Each of the conformational substates in sperm whale MbCO have different CO rebinding kinetics, where A_0 rebinds fastest and A_3 rebinds slowest.[3,9] So, the interactions of the bound ligand with the distal pocket residues play an important role in determining the barrier to CO binding with the heme iron.

Since identification of the dioxygen stretching frequency in MbO_2 has proven to be extremely complex,[22−27] it is still unclear whether similar conformational substates exist in MbO_2, and if so, whether they play a role in determining the barrier to oxygen binding. Thus, in order to help understand why the photoproduct yield decreases in oxymyoglobin at low pH, we examine the CO stretching frequency as a probe of distal pocket structure as a function of pH.

Figure 5 illustrates the A state FTIR spectra of horse skeletal muscle MbCO as a function of pH at 150 K. (The spectra remain unchanged below 150 K.) Over the pH range examined, only two substates are observed for horse MbCO—the A_1 and A_0 substates; the A_3 substate is not observed in the horse MbCO spectra. Above ca. pH 6.4, only the A_1 substate exists (1946 cm^{-1}). As the pH is decreased, the A_0 state becomes populated, as evidenced by the appearance of the A_0 band at 1961 cm^{-1}. Below pH 4.8, only the A_0 state is populated. Figure 3 demonstrates the pH-dependence of the A_1 state fraction, $A_1/(A_1 + A_0)$ and compares it to the pH-dependence of the MbO_2 photoproduct yield. As can be seen from Figure 3 (open squares versus closed circles), the pH-dependencies of (1) the A_1 state

(21) Quillin, M. L.; Arduini, R. M.; Olson, J. S.; Phillips, G. N. *J. Mol. Biol.* **1993**, *234*, 140.

(22) Miller, L. M.; Chance, M. R. *Biochemistry* **1995**, *34*, 10170.

(23) Maxwell, J. C.; Volpe, J. A.; Barlow, C. H.; Caughey, W. S. *Biochem. Biophys. Research Commun.* **1974**, *58*, 166.

(24) Potter, W. T.; Tucker, M. P.; Houtchens, R. A.; Caughey, W. S. *Biochemistry* **1987**, *26*, 4699.

(25) Bruha, A.; Kincaid, J. R. *J. Am. Chem. Soc.* **1988**, *110*, 6006.

(26) Proniewicz, L. M.; Kincaid, J. R. *J. Am. Chem. Soc.* **1990**, *112*, 675.

(27) Miller, L. M.; Chance, M. R. *J. Am. Chem. Soc.* **1994**, *116*, 9662.

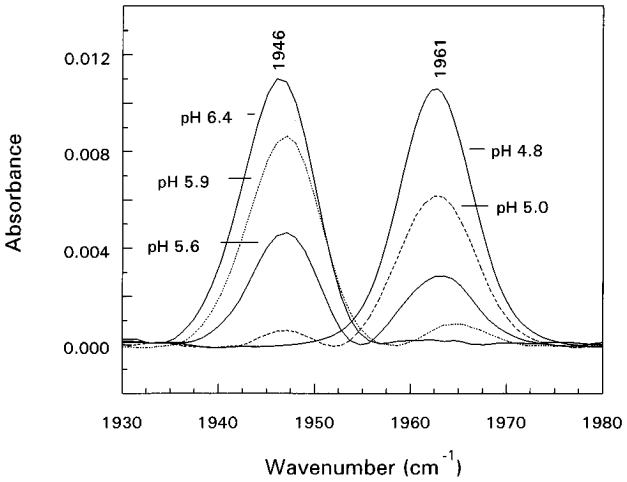

Figure 5. pH-dependence of the FTIR spectra of MbCO at 150 K (and below). Samples were 5 mM in 100 mM potassium phosphate buffer. The solvent was 75:25 by volume glycerol/buffer and sample thickness was 0.0025 cm. For each spectrum, 256 scans were taken at 2-cm^{-1} resolution and referenced to air.

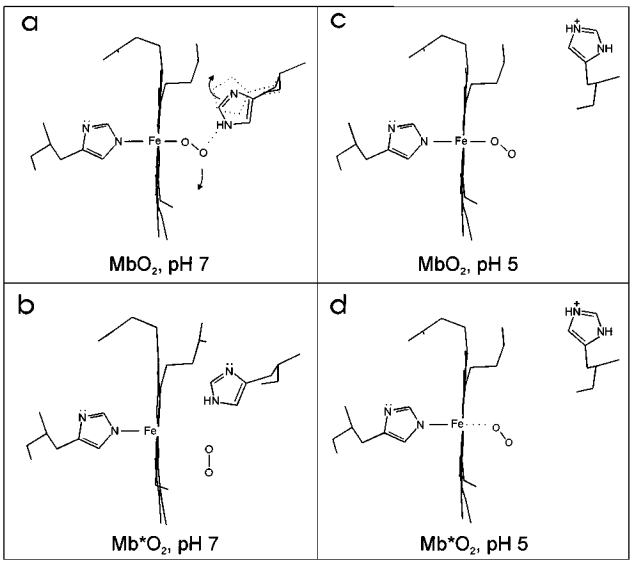

Figure 6. Proposed relationship between the dioxygen ligand and the distal histidine in the ligand-bound and photoproduct states at pH 7 versus pH 5. (a) At pH 7, the dioxygen ligand is hydrogen bonded to the distal histidine. (b) Upon photolysis, redistribution of electron density occurs, where the dioxygen ligand loses its polarity, and the hydrogen bond between the distal histidine and dioxygen is ruptured. Since the unbound ligand and the distal histidine are within the van der Waals distance of each other, the distal histidine and dioxygen push away from each other. (c) Conversely, at pH 5 in ligand-bound MbO_2, the distal histidine is thought to rotate about its $C^{\alpha}-C^{\beta}$ bond out of the distal pocket and toward the solvent, so that the dioxygen ligand is no longer within hydrogen bonding distance of the distal histidine. In this case, the distal histidine and the dioxygen ligand are further separated and no longer repel each other upon photolysis. (d) Thus, the dioxygen ligand may not be "pushed" as far away from the iron by the distal histidine, facilitating a lower barrier to rebinding.

population for MbCO and (2) the low-temperature photoproduct yield of MbO_2 are superimposable. This suggests that the conformational changes that give rise to the $A_1 \rightarrow A_0$ transition in MbCO are functionally important in determining the inner barrier to oxygen binding.

FTIR studies on distal histidine mutants of MbCO have demonstrated that the pH-dependence of the $A_1 \rightarrow A_0$ transition in MbCO is due to the titration of the distal histidine.[28,29] Although multiple substates are sometimes observed when the distal histidine is replaced by other amino acids, the A states of these mutants do not display a pH-dependence. In this work, we show that the mutant Mb(H64Q)O_2, where the distal histidine is replaced by a glutamine, does not show a pH-dependence of the photoproduct yield (Figure 3). This result supports the theory that the $A_1 \rightarrow A_0$ transition is dependent on the distal histidine.

It has been well-established that there is a hydrogen bond between dioxygen and the distal histidine at neutral pH. Champion and co-workers[18] have recently applied an "open" and "closed" distal pocket conformer theory to MbO_2, where they assume the hydrogen bond between the dioxygen ligand and the distal histidine is present only in the closed state; this feature is absent in the open state (Figure 6) and accounts for a $10^{3\pm2}$ increase in the value for k_{off} for this state. Using infrared difference spectra of isotopically labeled MbO_2, Potter et al.[24] have also suggested two conformational substates for MbO_2—a non-hydrogen-bonded (NHB) conformation and a hydrogen-bonded (HB) conformation with dioxygen stretching frequencies which fall at ~1150 and ~1125 cm^{-1}, respectively. Additionally, studies involving photolyzed/unphotolyzed difference FTIR spectra by our group[22,27] have revealed only a single, photolyzable dioxygen stretching frequency at 1131 cm^{-1}, similar to the HB conformation identified by Potter et al. The seeming inconsistency between the two infrared studies may indicate that the HB conformation has a higher barrier to recombination, so that it does not rebind at 10 K (making it "photolyzable"), whereas the NHB conformation has a much lower barrier to rebinding; thus, it appears "unphotolyzable". The decrease in photoproduct yield that we observe at low pH supports conformational changes that increase the NHB population as pH is decreased.

How do the conformational changes in the distal pocket associated with the HB → NHB transition promote a lower barrier for O_2 binding to the heme iron? Kinetics studies have shown that the polarity of the distal residue significantly affects the barrier to O_2 binding.[1,30,31] Carver et al.[1] have proposed that water molecules may hydrogen bond to a polar distal residue after photolysis, and displacement of this water is required for O_2 rebinding, thus increasing the inner rebinding barrier. When the distal histidine is replaced by an apolar residue, the bimolecular rate of ligand entry into the distal pocket is increased, as is the geminate rebinding rate. Additionally, Carlson et al. have shown that replacement of both the distal histidine and Val 68 with smaller residues relieves hindrance near the iron, promoting very rapid geminate rebinding of CO, NO, and O_2.

It is unlikely that solvent dynamics, i.e. the displacement of water molecules hydrogen bonded to the distal histidine, lead to the pH-dependence of the photoproduct yield at cryogenic temperatures. Instead, we proposed that pH-dependent structural changes in the distal pocket lead to the decreased O_2 geminate rebinding barrier at low pH in the following way: At pH 7 in ligand-bound MbO_2, the Fe−O−O moiety is significantly polarized toward an $Fe^{III}-O_2^-$structure[22,32−36] and the distal

(28) Braunstein, D. P.; Chu, K.; Egeberg, K. D.; Frauenfelder, H.; Mourant, J. R.; Nienhaus, G. U.; Ormos, P.; Sligar, S. G.; Springer, B. A.; Young, R. D. *Biophys. J.* **1993**, *65*, 2447.

(29) Li, T.; Quillin, M. L.; Phillips, G. N.; Olson, J. S. *Biochemistry* **1994**, *33*, 1433.

(30) Rohlfs, R. J.; Mathews, A. J.; Carver, T. E.; Olson, J. S.; Springer, B. A.; Egeberg, K. D.; Sligar, S. G. *J. Biol. Chem.* **1990**, *265*, 3168.

(31) Carlson, M. L.; Regan, R.; Elber, R.; Li, H.; Phillips, G. N.; Olson, J. S.; Gibson, Q. H. *Biochemistry* **1994**, *33*, 10597.

(32) Hoffman, B. M.; Petering, D. H. *Proc. Natl. Acad. Sci. U.S.A.* **1970**, *67*, 637.

histidine is situated in the heme pocket—close enough to the negatively charged dioxygen ligand to form a hydrogen bond (Figure 6a). Upon photolysis, redistribution of electron density occurs, such that the dioxygen ligand loses its polarity and, thus, the hydrogen bond with the distal histidine is ruptured in the photoproduct state. Since the unbound ligand and the distal histidine are within the van der Waals distance of each other (2.8 Å), the distal histidine and dioxygen push away from each other (Figure 6b). This "pushing away" of the dioxygen ligand may inhibit rebinding.

The "pushing-away" between the ligand and the distal histidine upon photolysis is supported by the recently published crystal structure of the MbCO photoproduct at pH 9 and 20 K.[37] In the ligand-bound state, the O atom of the CO ligand is 2.8 Å from the N_ϵ of the distal histidine. Upon photolysis, the distal histidine swings out of the distal pocket, and the CO ligand moves away from it, so that the photodissociated CO ligand sits in the center of the distal pocket. It is located 3.6 Å from the heme iron and also 3.9 Å from the N_ϵ of the distal histidine.[37]

However, the distal pocket structure is pH-dependent. At pH 5 in ligand-bound MbO_2, the distal histidine is thought to rotate about its $C^\alpha-C^\beta$ bond out of the distal pocket and toward the solvent, so that the dioxygen ligand is no longer within hydrogen-bonding distance of the distal histidine (Figure 6c). In this case, the distal histidine and the dioxygen ligand are further separated and no longer repel each other upon photolysis. Thus, the trajectory of the dioxygen ligand is different at pH 5, where the ligand may not be "pushed" as far away from the iron by the distal histidine (Figure 6d). This may facilitate rebinding.

Room temperature rebinding kinetics and molecular dynamics simulations of several distal pocket myoglobin mutants have alluded to different ligand trajectories upon photolysis, dependent on both the steric and electronic structure of the distal pocket.[1,2,4,38,39] The results presented here provide experimental data consistent with these findings and provide a direct measure of how ligand trajectory influences the inner barrier to oxygen binding in myoglobin. Future photoproduct yield studies involving site-directed distal pocket mutants of MbO_2 will be useful in mapping out the pathway for ligand binding from the distal pocket to the heme iron.

Different ligand trajectories is a likely structural interpretation of our data. However, our data do not rule out the possibility that pH affects the *electronic* structure of the heme-O_2 environment, such that the NHB state promotes relaxation of the photoproduct state to the ground state without complete bond lysis. There is ample evidence demonstrating a pH-dependence to the distal pocket structure which may affect the distribution of electron density throughout the Fe−O−O moiety. For example, protonation of the distal histidine adds a positive charge to the distal pocket. It may result in rotation of the distal histidine out of the distal pocket, also allowing water to enter. Thus, it is feasible that (1) the absence of the hydrogen bond between the dioxygen ligand and the distal histidine and/or (2) the presence of a positive charge in the low-pH distal pocket and/or (3) water in the distal pocket may result in redistribution of electron density throughout the metal−porphyrin π-electron system, resulting in a photoexcited state where the Fe−O bond is not ruptured. Once again, future photoproduct yield studies with site-directed distal pocket mutants of MbO_2 will help determine which distal pocket structural features influence the inner barrier to O_2 rebinding.

At this point, a note must be made about earlier studies by Doster et al.,[3] which do not show a pH-dependence of the geminate barrier to oxygen rebinding. These observations did not address the pH-dependence of the photoproduct yield. Those kinetic studies only probed rebinding rates assignable to long-lived (post-nanosecond) states, i.e. the "photolyzable" fraction of the entire MbO_2 distribution. As pH decreases, the photolyzable fraction decreases, but the oxygen rebinding barrier of the observed fraction is not affected. However, the entire distribution includes the unphotolyzable fraction, which increases at low pH, and has a lower rebinding barrier.

Finally, we address the pH-dependence of the low-temperature photoproduct yield for cobalt-substituted oxymyoglobin. Both the maximum and the minimum photoproduct yields for MbO_2 and $CoMbO_2$ are the same, and the shape of the $CoMbO_2$ titration curve strongly resembles that of MbO_2. These factors suggest that a similar HB ⇀ NHB transition occurs in $CoMbO_2$ as in MbO_2. Unfortunately, an analogous experiment with the A states of "CoMbCO" is not possible because CoMb does not bind CO.

One obvious difference exists between the $CoMbO_2$ and MbO_2 titration curves: The apparent pK of this titration curve for $CoMbO_2$ is 4.6, which is considerably lower than that of native MbO_2. This shift implies a difference in the distal pocket environments for the two species. More specifically, a lower apparent pK for $CoMbO_2$ indicates that protonation of the δ-nitrogen of the distal histidine is more difficult than for MbO_2. This may indicate a more-tightly-bound proton on the ϵ-nitrogen of the distal histidine; which, in turn, may result from a weaker hydrogen bond between dioxygen and the ϵ-nitrogen proton in $CoMbO_2$ when compared to MbO_2. A shift in pK by 1.1 units between the two species corresponds to a free energy difference of ~1.5 kcal/mol ($\Delta\Delta G = -2.303RT*\Delta pK$). This is small when compared to the overall stabilizing free energy of the HB state over the NHB state, which is 6 to 8 kcal/mol. Regardless, this seemingly small difference in hydrogen bond strength actually ***stabilizes*** $CoMbO_2$ with respect to MbO_2 at pH 5 because it causes the HB ⇀ NHB transition to occur at a lower pH.

This difference in hydrogen bond strength between the two species does not have an affect on the inner barrier to oxygen binding, i.e. the photoproduct yield for $CoMbO_2$ and MbO_2 is identical at pH 7, when the hydrogen bond is present. However, a weaker hydrogen bond to the distal histidine in $CoMbO_2$ may be a contributing factor to the ~300-fold increase[40] in the value of k_{off} for $CoMbO_2$ versus MbO_2 at pH 7. These results support other differences in the distribution of electron density throughout the Co−O−O and Fe−O−O moieties that may affect k_{off} for MbO_2 and $CoMbO_2$, either independently or by influencing the strength of the distal-side hydrogen bond (Figure 7).[22] For example, resonance Raman studies of $CoMbO_2$ and MbO_2[41,42] and cobaltous and ferrous porphyrin model compounds[43,44] have

(33) Yonetani, T.; Yamamato, H.; Iizuka, T. *J. Biol. Chem.* **1974**, *249*, 2168.
(34) Ikeda-Saito, M.; Iizuka, T.; Yamamato, H.; Kayne, F. J.; Yonetani, T. *J. Biol. Chem.* **1977**, *252*, 4882.
(35) Hori, H.; Ikeda-Saito, M.; Leigh, J. S. J.; Yonetani, T. *Biochemistry* **1982**, *21*, 1431.
(36) Lee, H. C.; Ikeda-Saito, M.; Yonetani, T.; Maggliozo, R. S.; Peisach, J. *Biochemistry* **1992**, *31*, 7274.
(37) Schlichting, I.; Berendsen, J.; Phillips, G. N.; Sweet, R. M. *Nature* **1994**, *371*, 808.
(38) Jongeward, K. A.; Magde, D.; Taube, D. J.; Marsters, J. C.; Traylor, T. G.; Sharma, V. S. *J. Am. Chem. Soc.* **1988**, *110*, 380.
(39) Jewsbury, P.; Kitagawa, T. *Biophys. J.* **1995**, *68*, 1283.
(40) Yamamoto, H.; Kayne, F. J.; Yonetani, T. *J. Biol. Chem.* **1974**, *249*, 691.
(41) Tsubaki, M.; Yu, N. T. *Proc. Natl. Acad. Sci. U.S.A.* **1981**, *78*, 3581.
(42) Tsubaki, M.; Srivastava, R. B.; Yu, N. T. *Biochemistry* **1982**, *21*, 1132.
(43) Walters, M. A.; Spiro, T. G.; Suslick, K. S.; Collman, J. P. *J. Am. Chem. Soc.* **1980**, *102*, 6857.

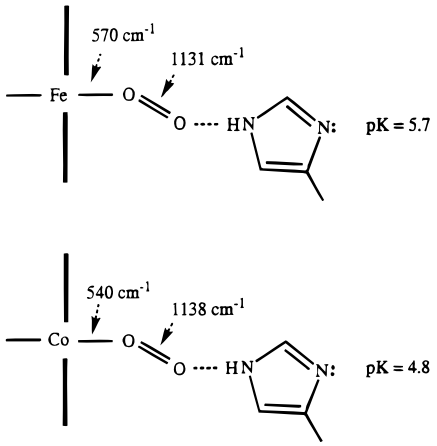

Figure 7. Comparison of the metal−oxygen and dioxygen stretching frequencies and distal histidine apparent p*K*'s for $CoMbO_2$ and MbO_2.

demonstrated that ν(Co−O) is lower than ν(Fe−O), suggesting weaker Co−O versus Fe−O bonds. In addition, a comparison of the dioxygen stretching frequencies of $CoMbO_2$ (1138 cm^{-1})[22] and MbO_2 (1131 cm^{-1})[22] to cobaltous (1150 cm^{-1}) and ferrous (1159 cm^{-1}) "picket fence" porphyrins,[45,46] where the distal side hydrogen bond is absent, reveals that the dioxygen stretching frequency of $CoMbO_2$ is much closer to the non-hydrogen bonded model compound than the corresponding ferrous species. Finally, the reduction in oxygen affinity in $CoMbO_2$ mutants where the distal histidine is replaced by apolar amino acids is slightly weaker than the ferrous species.[47] These results all support the photoproduct yield results which suggest a weaker hydrogen bond to the distal histidine in $CoMbO_2$ versus MbO_2.

Conclusions

In summary, the decrease in the low-temperature photoproduct yields at low pH for MbO_2 and $CoMbO_2$ implies (further) population of a conformational substate with a very lower barrier to oxygen binding. A comparison of the pH-dependence of (1) the photoproduct yield for oxymyoglobin and (2) the A_1 state of MbCO indicates that the distal pocket conformational change that gives rise to the $A_1 \rightarrow A_0$ state change in MbCO is functionally important in determining the inner barrier to oxygen binding. Thus, the conformational change that gives rise to the A_0 conformation lowers the barrier for both CO and O_2 binding. Since the pH-dependence of the MbO_2 photoproduct yield follows the same titration curve as the MbCO A state population, this suggests that this conformational change involves the distal histidine. This hypothesis is supported by the absence of a pH-dependence of the photoproduct yield for the mutant, Mb(H64Q)O_2. In MbO_2, we have assigned this conformational change to a transition between a hydrogen-bonded (HB) and non-hydrogen-bonded (NHB) form. The NHB state has a lower barrier to oxygen rebinding, which may be due to a photolyzed ligand that is situated very close to the iron atom because it is not pushed away by the distal histidine in its low pH conformation. The NHB state may also have a low barrier due to electronic differences in the distal pocket which alter the distribution of electron density throughout the Fe−O−O moiety. Finally, the pH-dependence of the photoproduct yield for MbO_2 versus $CoMbO_2$ supports evidence for electronic differences between the Fe−O−O and Co−O−O moieties. We observe a direct communication between the π-system of the porphyrin, through the dioxygen ligand, to the distal residue, where these differences in electron density distribution suggest a weaker hydrogen bond to the distal histidine in $CoMbO_2$.

Acknowledgment. We gratefully thank Dr. Joel Friedman and Dr. John Olson for insightful discussions, Dr. Caroline Lee for the cobalt-substituted myoglobin samples, and Dr. Maseo Ikeda-Saito for the human myoglobin mutant, Mb(H64Q)O_2. This research is supported by the National Institutes of Health (HL-45892). M.R.C. is the recipient of the Joseph and Anne Wunsch fellowship in Biophysical Engineering from the Albert Einstein College of Medicine. M.P. was supported by the Albert Einstein College of Medicine Summer Undergraduate Research Program.

JA952534J

(44) Proniewicz, L. M.; Bruha, A.; Nakamoto, K.; Kyuno, E.; Kincaid, J. R. *J. Am. Chem. Soc.* **1989**, *111*, 7050.
(45) Collman, J. P.; Brauman, J. I.; Halbert, T. R.; Suslick, K. S. *Proc. Natl. Acad. Sci. U.S.A.* **1976**, *73*, 3333.
(46) Collman, J. P.; Gagne, R. R.; Reed, C. A.; Halbert, T. R.; Lang, G.; Robinson, W. T. *J. Am. Chem. Soc.* **1975**, *97*, 1427.
(47) Ikeda-Saito, M.; Lutz, R. S.; Shelley, D. A.; McKelvey, E. J.; Mattera, R.; Hori, H. *J. Biol. Chem.* **1991**, *266*, 23641.